

# Simulation Experiments of Supercells and Tatsumaki along Typhoon Rainbands

Kazuhisa Tsuboki

Hydrospheric Atmospheric Research Center

Nagoya University

Furo-cho, Chikusa-ku, Nagoya 464-8601, Japan

e-mail: [tsuboki@rain.hyarc.nagoya-u.ac.jp](mailto:tsuboki@rain.hyarc.nagoya-u.ac.jp)

## Abstract

Even through a typhoon center is located in the far distance, a disaster due to a strong wind is occasionally caused by a “tatsumaki” which is a tornado in Japan. When Typhoon 0613 (T0613) moved northward off the west of Kyushu, a severe disaster was caused by an intense tatsumaki along the east coast of Kyushu. The tatsumaki occurred when typhoon rainbands moved northward along the east coast. Two simulations with different horizontal resolutions were performed using the Cloud Resolving Storm Simulator (CReSS) Ver.2.2 in the present study. The experiment with a horizontal resolution of 500m successfully simulated not only the overall structure and movement of T0613 but also a detailed structure of the typhoon rainbands. The other experiment with a resolution of 75 m simulated that a tatsumaki forms in convective clouds. The result shows that the outermost rainband was composed of supercells which involve a meso-cyclone. Tatsumakis form within the supercells. The vorticity of the tatsumaki attains  $0.9 \text{ s}^{-1}$  and wind speed is larger than  $70 \text{ m s}^{-1}$ . On the basis of the result, we will discuss the relationships between rainbands, convective clouds and tatsumakis.

## 1. Introduction

Tornadoes and waterspouts are a violently rotating air below a convective cloud. They are called “tatsumaki” in Japan. Niino et al. (1997) reported that 20.5 tornadoes and 4.5 waterspouts occur on average in Japan and that about 20 % of tornadoes occur in association with typhoons. Strong wind is caused by not only typhoons but also associated tatsumakis. Even though a typhoon center is at a distance, a tatsumaki occasionally causes severe wind. An intense tatsumaki occurred in Nobeoka City to the far east of the center of Typhoon 0613 (T0613) on September 17, 2006. Using a cloud resolving model, we studied clouds and tatsumakis along typhoon rainbands.

We have been developing the cloud-resolving model named the “Cloud Resolving Storm Simulator” (CReSS) since 1998. CReSS is designed for parallel computers and was optimized for the Earth Simulator. Objectives of the model development are numerical simulations and high-resolution predictions of high-impact weather systems. A typhoon is one of high-impact weather systems in East Asia. It brings heavy rainfalls and strong winds, and often causes tatsumakis. Quantitative and accurate prediction of rainfall and wind is necessary for prevention/reduction of disasters associated with a typhoon.

In the present study, we performed a simulation experiment of T0613 and the associated tatsumaki using

the CReSS model to reveal structure of clouds along the typhoon rainband and the mechanism of the tatsumaki. The horizontal grid size is 500m in the simulation of the typhoon and the calculation domain is sufficiently large to simulate overall structure of the typhoon. A high-resolution experiment was performed to study the relationship between the supercells and the tatsumaki with a grid spacing of 75m.

Using the CReSS model, we performed high-resolution simulations of the typhoon and the tatsumaki. The purpose of the present study is to clarify structures of clouds along typhoon rainbands and the relationship between clouds and tatsumakis. Detailed structure of the tatsumaki will be examined using the result of the simulation of the tatsumaki.

## 2. Description of the CReSS model

The basic formulation of CReSS is based on the non-hydrostatic and compressible equation system using terrain-following coordinates. Prognostic variables are three-dimensional velocity components, perturbations of pressure and potential temperature, water vapor mixing ratio, sub-grid scale turbulent kinetic energy (TKE), and cloud physical variables. A finite difference method is used for the spatial discretization. The coordinates are rectangular and dependent variables are set on a

staggered grid: the Arakawa-C grid in horizontal and the Lorenz grid in vertical. For time integration, the mode-splitting technique is used. Terms related to sound waves of the basic equation are integrated with a small time step and other terms with a large time step.

Cloud physical processes are formulated by a bulk method of cold rain, which is based on Lin et al. (1983), Cotton et al. (1986), Murakami (1990), Ikawa and Saito (1991), and Murakami et al. (1994). The bulk parameterization of cold rain considers water vapor, rain, cloud, ice, snow, and graupel.

Parameterizations of the sub-grid scale eddy motions in CReSS are one-order closure of Smagorinsky (1963) or the 1.5-order closure with turbulent kinetic energy (TKE). In the latter parameterization, the prognostic equation of TKE is used. All numerical experiments of the present paper used the 3-dimensional 1.5-order closure scheme. The surface process of CReSS is formulated by a bulk method. The bulk coefficients are formulated by the scheme of Louis et al. (1981).

Several types of initial and boundary conditions are available. For a numerical experiment, a horizontally uniform initial field provided by a sounding profile will be used with an initial disturbance of a thermal bubble or random temperature perturbation. The boundary conditions are rigid wall, periodic, zero normal-gradient, and wave-radiation types.

CReSS enables to be nested within a coarse-grid model and to perform a prediction experiment. In the experiment, the initial field is provided by interpolation of grid point values and the boundary condition is provided by the coarse-grid model. For a computation within a large domain, conformal map projections are available. The projections are the Lambert conformal projection, the polar stereographic projection and the Mercator projection.

For parallel computing of a large computation, CReSS provides two-dimensional domain decomposition in horizontal. Parallel processing is performed using the Message Passing Interface (MPI). Communications between the individual processing elements (PEs) are performed by data exchange of the outermost two grids. The OpenMP is optionally available to be used.

The readers can find the more detailed description of CReSS in Tsuboki and Sakakibara (2001) or Tsuboki and Sakakibara (2002).

### 3. Observation of Typhoon 0613

T0613 was generated to the east of the Philippines on September 10, 2006 and moved westward with developing. It approached to the western Okinawa and turned to the north with its maximum intensity. After T0613 passed over Ishigaki Island, it moved northeastward. The center of T0613 landed on the northern Kyushu on September 17. When T0613 moved northeastward off the west coast of Kyushu, cloud band formed to the east of Kyushu (Fig. 1).

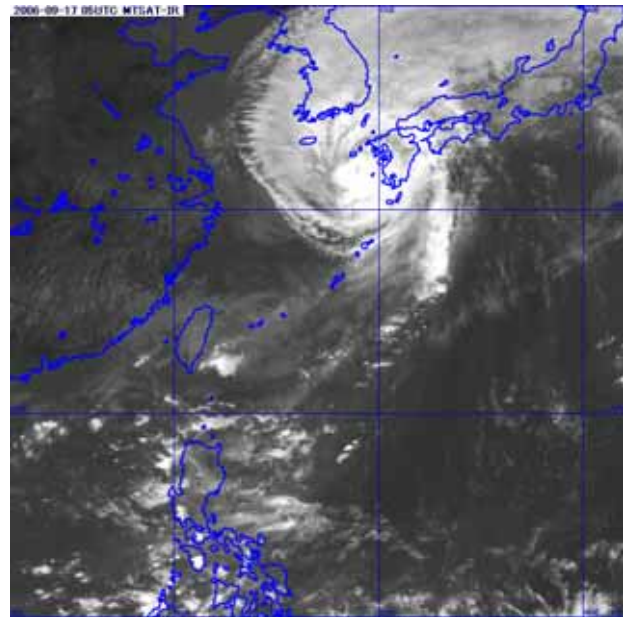


**Figure 1:** IR image of the MTSAT satellite at 0500 UTC September 17, 2006.

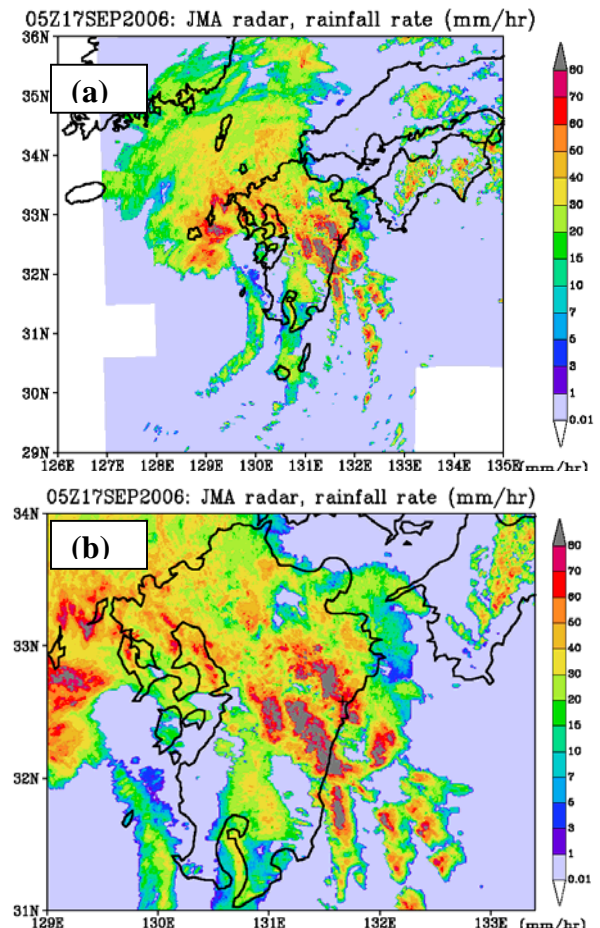


**Figure 2:** Rainfall distributions obtained from the JMA radar in (a) the western Japan and (b) the Kyushu region at 0500 UTC September 17, 2006.

The radar observation by the Japan Meteorological Agency (JMA) shows that the center of T0613 was located to the southwest of Kyushu and that 2 or 3 intense rainbands formed along the east coast of Kyushu (Fig. 2a). The rainbands are composed of intense convective clouds (Fig. 2b). They moved northward along the east coast of Kyushu.

The TRMM satellite observation showed a band of large precipitable water extended meridionally to the east of Kyushu (not shown).

The intense tatsumaki occurred in Nobeoka City which is indicated by the cross in Fig. 2b at 05UTC September 17, 2006. It killed three people and caused the train accident in Kyushu.

#### 4. Simulation of Typhoon 0613

Since the tatsumaki occurred along rainbands of T0613, an accurate simulation of the typhoon is necessary for the simulation of the tatsumaki. Using the CReSS model, the simulation experiment was performed with the experimental setting summarized in Table 1. We refer to the experiment as Exp-500m.

**Table 1: Experimental setting of the typhoon simulation.**

Domain	x: 896 km, y:896km, z:19.2km
Grid number	x: 1795, y:1795, z:67
Resolution	H: 500m, V:80 - 300m
Initial time	0000 UTC September 17, 2006
Integration time	6 hours
Microphysics	bulk cold rain type
Initial condition	JMA-Regional Spectral Model
Boundary condition	JMA-Regional Spectral Model
Surface	real topography and sst
Computer	the Earth Simulator (1024CPUs)

The movement and overall structure of T0613 are successfully simulated in Exp-500m. Figure 3 shows the horizontal display of the simulated T0613 in the all domain of the experiment at 0500 UTC September 17, 2007. The typhoon center is located at around 128.5E and 31.7N to the west of Kyushu. While the eye-wall is not significant, a strong wind is present around the center. Intense and long rainbands extend from the northern Kyushu to the south for about 400 km crossing the east coast of Kyushu at this time. Weak rainfall region is present to the north of Kyushu. The horizontal distribution of the rainfall simulated in Exp-500m is very similar to the observed rainfall distribution shown in Fig. 2a.

The close view of the rainbands (Fig. 4) shows that three rainbands are simulated to the east of Kyushu. The northernmost rainband and the middle rainband are merged into a single rainband over Kyushu. Another rainband is formed to the south of the these rainbands.

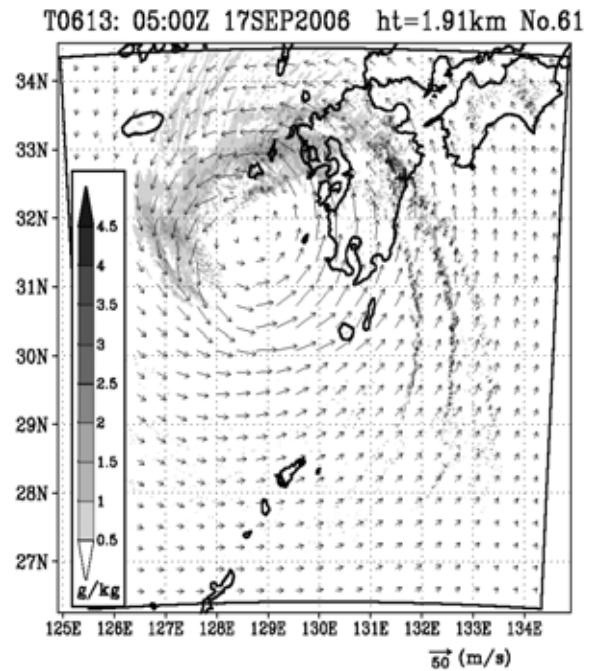


**Figure 3: Horizontal distribution of the mixing ratio of rain (gray levels;  $g\ kg^{-1}$ ) and horizontal wind (arrows) at 1.9km in height at 0500 UTC September 17, 2006 obtained from the CReSS 500m-resolution simulation.**

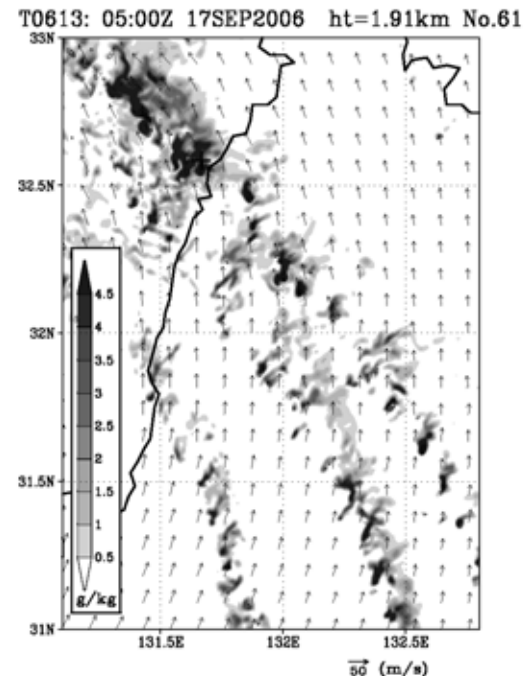


**Figure 4: Same as Fig. 3 but for the rainbands along the east coast of Kyushu.**

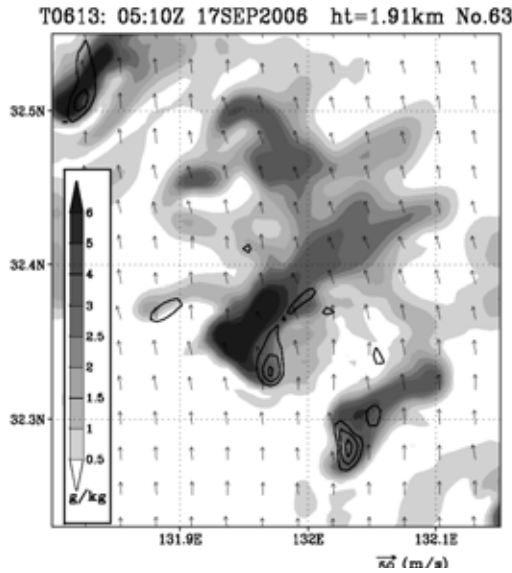


**Figure 5: Convective cell composing the rainband to the east of Kyushu simulated in the 500-resolution experiment: the mixing ratio of rain (gray levels;  $\text{g kg}^{-1}$ ), vertical vorticity (contours from  $0.01 \text{ s}^{-1}$  every  $0.01 \text{ s}^{-1}$ ), and horizontal wind (arrows) at 1.9km in height at 0510 UTC September 17, 2006**

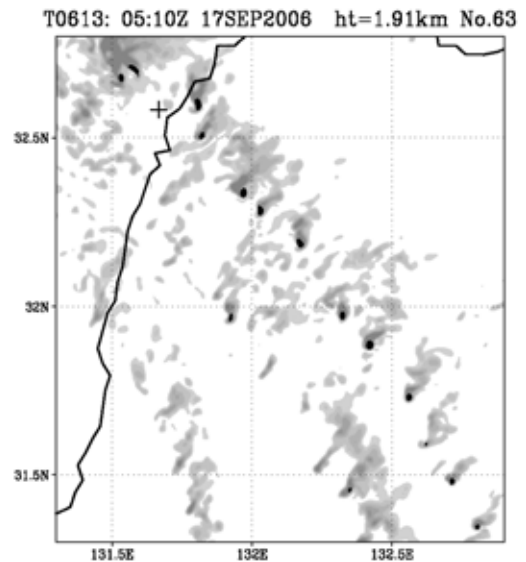


**Figure 7: Horizontal distribution of the Supercell Index (SCI) at a height of 1.9 km at 0510UTC September 17, 2006. The gray levels are mixing ratio of rain.**

in Fig. 2b very much.

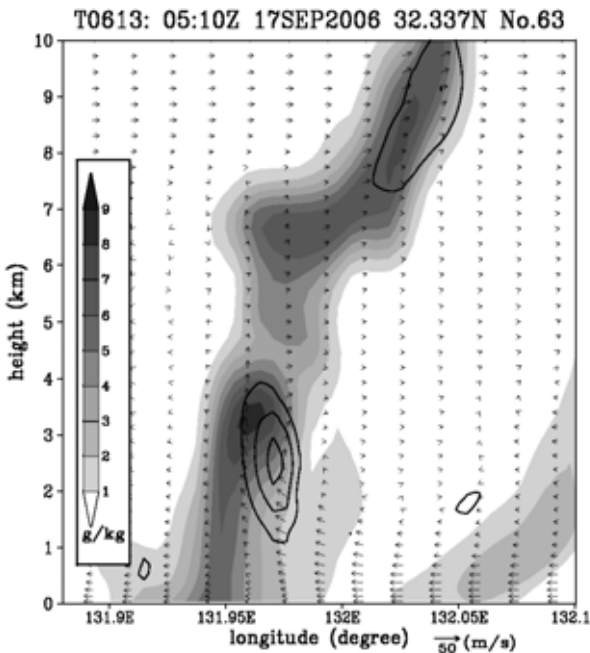
The simulation (Fig.4) shows that the rainbands are composed of convective cells. The enlarged display of convective cells at a height of 1.9km is shown in Fig. 5. The cell extends from the southwest to the northeast with a horizontal scale of 10km. A hook-shaped structure is found in the southern part of the cell. A large vertical vorticity of  $0.03 \text{ s}^{-1}$  is present in the part. This indicates that the convective cell is a supercell. Most cells formed along the typhoon rainbands to the east of Kyushu (Fig. 4) are supercell.

Figure 6 shows the vertical cross-section of the convective cell in Fig. 5 in the zonal direction. The convective cell reaches to a height of 10 km and mixing ratio of precipitation (rain, snow and graupel) are large in the cell below a height of 5 km. The intense vertical vorticity is present in the cell between 1 and 4 km in height where the vertical velocity is large. The intense vorticity was created by the tilting of horizontal vorticity in the intense upward motion. An intense precipitation occurred to the west of the strong upward motion and the upward motion is maintained. As a result, the supercell lasts for long time.

Since a large number of convective cells are simulated in the experiment of Exp-500m, we defined an index (*SCI*: the supercell index) to identify supercells as

$$SCI = \left( \frac{\partial v}{\partial x} - \frac{\partial u}{\partial y} \right) w.$$

Where  $u$ ,  $v$  and  $w$  are zonal, meridional and vertical velocity components at around a height of the mesocyclone in convective cells, respectively. In the present study, the height is 1.9 km and convective cells with *SCI* larger than 0.1 are identified as a supercell.



**Figure 6: Vertical cross section of the convective cell in the zonal direction at  $32.337^\circ\text{N}$ : the mixing ratio of precipitation (rain, snow and graupel (gray levels;  $\text{g kg}^{-1}$ ), vertical vorticity (contours from  $0.01 \text{ s}^{-1}$  every  $0.01 \text{ s}^{-1}$ ), and horizontal wind (arrows) at 0510 UTC September 17, 2006**

They correspond to the observed three rainbands shown

Horizontal distribution of *SCI* at 0510 UTC September 17 (Fig. 7) indicates that most convective cells along the northernmost rainband include an area of *SCI* larger than 0.1. This indicates that the outermost rainband is composed of supercells. In contrast, almost no area of *SCI* larger than 0.1 is found along the middle and southernmost rainbands. This indicates that the two rainbands have almost no supercells.

## 5. Simulation of the tatsumaki

The horizontal scale of tatsumaki is an order of a few 100 m in the present case. Grid size of model should be a few 10 m to simulate the tatsumaki. The experimental setting for the simulation of tatsumaki is summarized in Table 2. The experiment will be referred to as Exp-75m in this paper. The initial and boundary conditions are provided by the result of Exp-500m.

A detailed structure of the supercell which produced a tatsumaki was simulated (Fig. 8). The supercell extends the north-south direction with a horizontal length of 20 km. Intense rain occurred in the southern part of the supercell with a very sharp hook-shaped structure at the southernmost part. The tatsumaki is formed in the hook-shaped structure which is indicated by the circle in Fig. 8. A weak rain is present in the northern part of the cell.

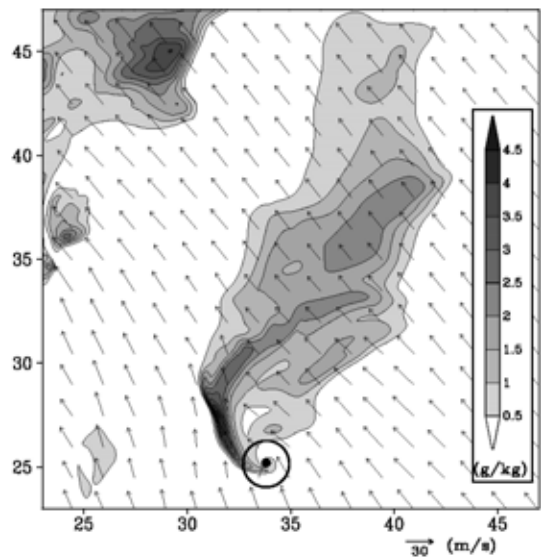


**Figure 8:** Horizontal display of the supercell at a height of 200m at 0500 UTC September 17, 2007 obtained from 75 m-resolution simulation. Gray levels are mixing ratio of rain ( $\text{g kg}^{-1}$ ) and arrows are horizontal velocity. The circle indicates the tatsumaki developed in the supercell.

**Table 2: Experimental setting of the tatsumaki simulation.**

Domain	x: 60 km, y:60km, z:19.2km
Grid number	x: 800, y:800, z:67
Resolution	H: 75m, V:80 - 300m
Initial time	0405 UTC September 17, 2006
Integration time	1.25 hours
Microphysics	bulk cold rain type
Initial condition	JMA-Regional Spectral Model
Boundary condition	JMA-Regional Spectral Model
Surface	real topography and sst
Computer	Hitachi SR11000

A close view of the southern part of the supercell (Fig. 9) shows that the tatsumaki forms inside of the hook. The horizontal scale of the simulated tatsumaki is about 300 m, which is the almost same scale with the observed tatsumaki. The experiment of Exp-75m successfully simulates the tatsumaki within the supercell. The maximum vorticity of the tatsumaki is  $0.9 \text{ s}^{-1}$  and pressure perturbation at the center is -27 hPa. The pressure field and the velocity field are in the cyclostrophic balance in a high accuracy. This is a most significant characteristic of the tatsumaki.

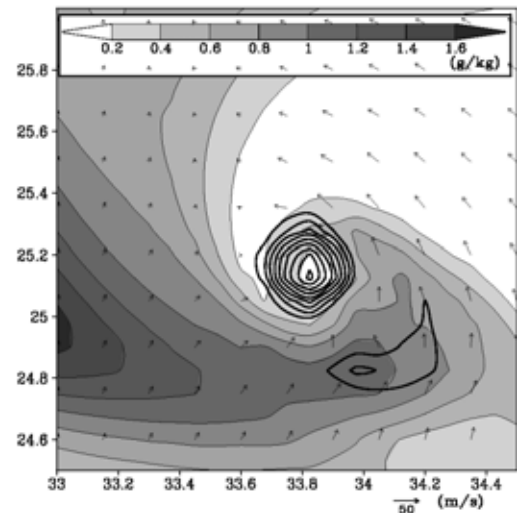


**Figure 9:** Enlarged view of the southernmost part of the supercell indicated by the circle in Figure 7. Gray levels are mixing ratio of rain ( $\text{g kg}^{-1}$ ), contours are vertical vorticity from  $0.1 \text{ s}^{-1}$  every  $0.1 \text{ s}^{-1}$  and arrows are horizontal velocity.

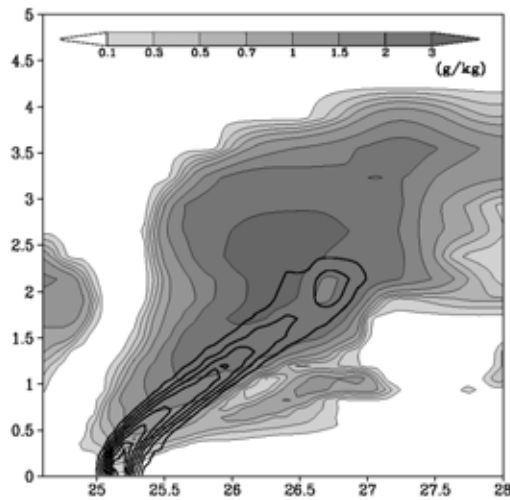


**Figure 10: Vertical cross section in the meridional direction at the center of the tatsumaki. Gray levels are mixing ratio of rain ( $\text{g kg}^{-1}$ ), contours are vertical vorticity from  $0.1 \text{ s}^{-1}$  every  $0.1 \text{ s}^{-1}$ .**

Figure 10 shows the vertical cross-section of the tatsumaki in Fig. 9 in the north-south direction. The vortex tube structure is significant in the cross-section. The tatsumaki tilted northward and reached to a height of 2 km in the cloud. The largest vorticity and pressure perturbation are present near the surface and decrease with height. Upward velocity is large around the tatsumaki with a maximum velocity of  $21 \text{ m s}^{-1}$  while the vertical motion within the tatsumaki is downward. As a result, cloud is lowered at the center of the tatsumaki to form a funnel structure.

The wind velocity around the tatsumaki is very large which resulted in the severe disaster in the Nobeoka City. The horizontal wind speed of the simulated tatsumaki is larger than  $70 \text{ m s}^{-1}$  on the east side of the tatsumaki while it is weak in the west side (Fig. 11). This asymmetry of horizontal wind speed well simulated the asymmetry of the damage distribution due to the tatsumaki. The damage is significant on the right-hand side of the pass of the tatsumaki while it is small on the left-hand side with the northward movement of the tatsumaki.

Another simulation experiment with a horizontal resolution of 75 m was performed within a much larger domain using the Earth Simulator. A preliminary result shows many tatsumakis were simulated along the typhoon rainbands. Most tatsumakis form along the northernmost (outermost) rainband. This is consistent with that the outermost rainband is composed of supercells in the experiment of Exp-500m.

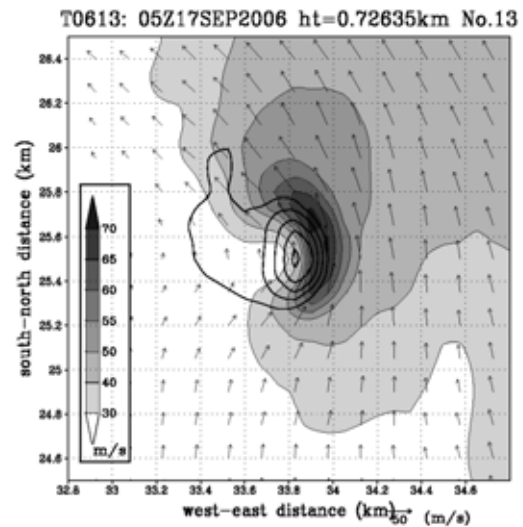


**Figure 11: Horizontal distribution of wind speed (gray levels;  $\text{m s}^{-1}$ ) at a height of 0.73km at 0500UTC September 17, 2006.**

## 6. Discussion

Since a tatsumaki forms in a very short time and its horizontal scale is quite small, observation of tatsumaki is very difficult. Tatsumaki is caused by a convective cloud which develops within a large-scale weather system such as a typhoon and a cold front. An accurate simulation of both the large-scale weather system and the convective cloud is necessary for simulation of tatsumaki. Such computation requires very high resolution and a large computational domain. A direct numerical prediction of tatsumaki is not possible at present.

Detection of a meso-cyclone within a convective cloud using Doppler radar is a feasible way for tatsumaki warning. Another feasible method to forecast a tatsumaki is simulation of convective clouds including the meso-cyclone using a cloud-resolving model. In this method, tatsumaki will not be predicted directly but a convective cloud which has a possibility to produce a tatsumaki is predicted. This is a sort of potential prediction of tatsumaki. Relationship between the cloud and the tatsumaki should be clarified for a successful prediction.

In the present study, the simulation experiment revealed that the northernmost rainband of T0613 consisted of supercells. The high resolution experiment showed many tatsumakis occurred along the rainband. A detailed examination of one of the supercell showed that the tatsumaki formed in the hook-shaped structure of the supercell in the southernmost part. These results indicate that the outermost rainband of typhoon includes dangerous convective clouds and tatsumakis are possible to occur in the outermost rainband.

## 7. Summary

Typhoons occasionally accompany tornadoes (tatsumakis in Japanese) and cause disasters due to strong winds. When the typhoon 0613 (T0613) approached the western Japan on September 17, 2006, it accompanied a severe tatsumaki. It killed three people and caused a train accident in Kyushu. We performed a simulation experiment of T0613 and the associated tatsumaki using the CReSS model to reveal structure of clouds along the typhoon rainbands. The horizontal grid size is 500m in the simulation of the typhoon and the calculation domain is sufficiently large to simulate overall structure of the typhoon. The initial condition (00 UTC September 17, 2006) and the boundary conditions were provided by the regional model (RSM) output of the Japan Meteorological Agency (JMA). We used 128 nodes of the Earth Simulator for the simulation.

The result of the simulation experiment at about 5 hours from the initial time showed that intense rainbands were formed in the eastern part of T0613. One of them passed over Nobeoka City at around 05 UTC September 17. This corresponds to the observation of JMA. Some clouds composing the rainband are intense supercells including a meso-cyclone.

A high-resolution experiment was performed to study the relationship between the supercells and the tatsumaki with a grid spacing of 75m. The result shows that hook-shaped structure forms in the southernmost part of the supercell and that the intense tatsumaki is simulated in the hook-shaped part of the supercell. The horizontal diameter of the tatsumaki is about 300m and its maximum vorticity is larger than  $0.9 \text{ s}^{-1}$ . Pressure perturbation is about -27 hPa at the center of the tatsumaki and maximum horizontal velocity reaches to  $70 \text{ m s}^{-1}$ . The tatsumaki extends up to a height of 2.5 km within the strong upward motion. The simulation showed the detailed structures of the tatsumaki and the supercell formed in the typhoon rainband.

## Acknowledgments

The Hydrospheric Atmospheric Research Center (HyARC) at Nagoya University has supported the development of the CReSS model as a research program since 2003. We used the mainframe computers and supercomputers at the University of Tokyo and Nagoya University for the development and calculations of the CReSS model. The Earth Simulator at the Earth Simulator Center was used for simulations and calculations using the CReSS model.

## References

- Cotton, W. R., G. J. Tripoli, R. M. Rauber and E. A. Mulvihill, 1986:  
Numerical simulation of the effects of varying ice crystal nucleation rates and aggregation processes on orographic snowfall.  
*J. Climate Appl. Meteor.*, **25**, 1658-1680.
- Ikawa, M. and K. Saito, 1991:  
Description of a nonhydrostatic model developed at the Forecast Research Department of the MRI.  
*Technical Report of the MRI*, 28, 238pp.
- Lin, Y. L., R. D. Farley and H. D. Orville, 1983:  
Bulk parameterization of the snow field in a cloud model.  
*J. Climate Appl. Meteor.*, **22**, 1065-1092.
- Louis, J. F., M. Tiedtke and J. F. Geleyn, 1981:  
A short history of the operational PBL parameterization at ECMWF.  
*Workshop on Planetary Boundary Layer Parameterization* 25-27  
Nov. 1981, 59-79.
- Murakami, M., 1990:  
Numerical modeling of dynamical and microphysical evolution of an isolated convective cloud - The 19 July 1981 CCOPE cloud.  
*J. Meteor. Soc. Japan*, **68**, 107-128.
- Murakami, M., T. L. Clark and W. D. Hall 1994:  
Numerical simulations of convective snow clouds over the Sea of Japan;  
Two-dimensional simulations of mixed layer development and convective snow cloud formation.  
*J. Meteor. Soc. Japan*, **72**, 43-62.
- Niino, H., T. Fujitani, and N. Watanabe, 1997:  
A Statistical Study of Tornadoes and Waterspouts in Japan from 1961 to 1993  
*J. Climate*, **10**, 1730-1752.
- Smagorinsky, J., 1963:  
General circulation experiments with the primitive equations. I. The basic experiment.  
*Mon. Wea. Rev.*, **91**, 99-164.
- Tsuboki, K. and A. Sakakibara, 2001: CReSS User's Guide 2nd Edition, 210p.
- Tsuboki, K. and A. Sakakibara, 2002:  
Large-scale parallel computing of Cloud Resolving Storm Simulator.  
*High Performance Computing, Springer*; H. P. Zima et al. Eds, 243-259.